complicated. Nevertheless, it is useful to estimate the damping of our resonant oscillations using a simple physical model which is well known[13] to describe the Landau damping effect in a homogeneous plasma. Consider a density perturbation which for the moment is stationary in space (Fig. 3). After a time $(k_xW)^{-1}$, the perturbations having a wavelength of $2\pi/k_x$ will be "dissipated" by the thermal motion W. We now let the perturbations oscillate with a period of ω^{-1}. Evidently, the damping effect due to temperature motion (Landau damping) is not important if the dissipation time $(k_xW)^{-1}$ is long compared to the oscillation period ω^{-1}:

$$\omega \gtrsim k_xW. \tag{4.1}$$

[13] M. N. Rosenbluth, Danish Atomic Energy Commission, Risø Report No. 18, 1960, p. 197 (unpublished).

Let $k_x=2\pi/\lambda_x$ with $\lambda_x=2\partial x_t/\partial n$, and make use of (3.2) and (3.3) with $\omega_c=0$. (4.1) can be reduced to

$$\{1+\omega_p{}^2(0)/[\omega^2-\omega^2{}_p(0)]\}^{1/2}\gtrsim 1, \tag{4.2}$$

where $\omega^2{}_p(0)$ is the plasma density at the wall. This inequality is certainly not strong and in fact the equality sign is valid for zero wall density. According to this estimate, therefore, thermal damping effects cannot be excluded and a further investigation is physically significant.

ACKNOWLEDGMENTS

I would like to thank Professor N. Herlofson, Dr. A. Dattner, and Dr. P. Weissglass for useful discussions.

PHYSICAL REVIEW VOLUME 133, NUMBER 4A 17 FEBRUARY 1964

Fermi Surface of Ferromagnetic Nickel*

J. C. PHILLIPS†

Department of Physics and Institute for the Study of Metals, University of Chicago, Chicago, Illinois

(Received 3 June 1963; revised manuscript received 21 October 1963)

A survey of nonmagnetic band structures near the top of the 3*d* band is made. The aim is to combine these band structures with a wide variety of experimental data to determine the exchange splittings of the *d* bands ΔE_{dd} and the *s-p* conduction band ΔE_{ss}. Saturation magnetization, *g* factors, and high-field Hall data are analyzed and compared with the effect of *s-d* hybridization on the number of *s* electrons. One concludes that if the neck observed in magnetoresistance studies is associated with the same band edge as the Cu neck, $\Delta E_{dd}\lesssim 0.8$ eV. It appears that $\Delta E_{ss}\lesssim\Delta E_{dd}/2$. Recent optical rotation data of Krinchik are interpreted as giving a direct measurement of ΔE_{dd}. The value obtained is (0.6 ± 0.1) eV, in good agreement with the values obtained from other data.

1. INTRODUCTION

ENORMOUS progress has been made recently in extending our knowledge of the electronic structure of metals through a variety of experiments which determine certain properties of the Fermi surface.[1] Fawcett and Reed have recently studied the transverse magnetoresistance and Hall coefficient of Ni.[2,3] By combining their results with the results of saturation magnetization,[4] gyromagnetic resonance,[4] and Faraday rotation measurements,[5] it may be possible to obtain a rather precise picture of certain portions of the Fermi surface of ferromagnetic Ni.

Before undertaking an analysis of the experimental data we must make certain assumptions about the band structure of Ni. All Fermi surface measurements tend to be almost too microscopic. Because the measurements are confined to the neighborhood of $E=E_F$, one views the band structure through a slit that is energetically very narrow. Many different band models of $\mathrm{E}_n(\mathbf{k})$, where n labels bands, often fit the same data with apparently equal success. It is therefore necessary at the outset to attempt to define certain rules for physically plausible band structures. If the rules are correct, reasonable models which fit experiment naturally will emerge from the analysis.

For nontransition metals this prescription has been carried through with great success by Harrison.[6] His rule is to apply the nearly free-electron model. Ashcroft[7] has extended the pseudopotential treatment to characterize allowed Fermi surface topologies. We know that narrow *d* bands cannot be treated in this fashion, and

* Supported in part by the National Science Foundation.

† Guggenheim Fellow with a grant-in-aid from the Sloan Foundation.

[1] *The Fermi Surface*, edited by W. A. Harrison and M. B. Webb (John Wiley & Sons, Inc. New York, 1960).

[2] E. Fawcett and W. A. Reed, Phys. Rev. Letters **9**, 336 (1962).

[3] E. Fawcett and W. A. Reed, Phys. Rev. **131**, 2463 (1963).

[4] C. Kittel, *Introduction to Solid State Physics* (John Wiley & Sons, Inc., New York, 1953), pp. 166–171.

[5] G. S. Krinchik and R. D. Naralieva, Zh. Eksperimic Teor. Fiz. **36**, 1022 (1959) [translation: Soviet Phys.—JEPT **36**, 724 (1959)]. G. S. Krinchik and A. A. Gorbacher, Fiz. Metal. i Metalloved. **11**, 203 (1961).

[6] W. Harrison, Ref. 1, p. 28.

[7] N. W. Ashcroft, Phys. Letters **4**, 292 (1963).

this has so far discouraged theorists from treating transition metals.

The general shape of d bands, especially near the top, is found to be nearly the same in all calculations (see Sec. 2). The technical problem one then faces is twofold. Because the absolute position of the d bands is sensitive to small changes in the crystal potential that have little effect on the s-p conduction bands, one must adjust the relative positions of these bands for both ↑ and ↓ spins. One must also place the Fermi energy consistently for each spin. Because of the crossing or hybridizing between the conduction band and d bands, this appears to be quite difficult.

An accurate solution of this problem can be carried out by first decoupling the d bands and conduction bands. The density of states in the conduction band alone or the d band alone has been calculated by several workers. Using their results we can place E_F with some precision for ↑ and ↓ bands. We also note that a *single d* band is quite narrow (~1 eV) compared to the conduction band width (~10 eV). If we neglect the former compared to the latter then the Anderson compensation theorem[8] allows us to conclude that s-d hybridization will not shift E_F appreciably from its decoupled value.

Band calculations show that the d bands of Ni are quite similar to those of Cu, apart from broadening and a shift relative to the $s-p$ conduction bands. This enables one, e.g., to consider unmagnetized Ni as a chemically shifted version of Cu. The band structure of Cu is well known through Fermi surface studies[1] and band calculations[9,10] and this gives us additional confidence in treating Ni.

In Sec. 2 we survey calculations of d bands to extract features in the energy range relevant to Ni. We discuss these features in general terms, in order to rely as little as possible on the details of the calculations. In later sections we analyze the data and characterize two alternative models which are distinguishable experimentally.

2. SURVEY OF CALCULATED fcc d BANDS

Band calculations have always suggested that the d-band shape can be fit moderately well with tight-binding secular equations, the nearest-neighbor overlap integrals being treated as parameters.[11] There is no experimental evidence at present to indicate whether this approach is sufficiently precise to determine the Fermi surface of Ni. We adopt a somewhat more general approach here to the levels near the top of the d band.

Consider the highest states at Γ, X, L, and W (Γ_{12}, X_5, $W_{1'}$, and L_3, respectively). For the fcc structure these have been calculated for atomic potentials corresponding to Cu,[9,10] Fe,[12] and Ni.[13,14] The energies are listed in Table I. We define the radial width ΔE_r as the difference in energy between Γ_{12} and X_5 or $W_{1'}$, whichever is higher and the angular width ΔE_θ as the corresponding difference with Γ_{12} replaced by L_3. The ratio of these widths is

$$\varphi=\Delta E_r/\Delta E_\theta, \tag{2.1}$$

which provides a measure of the band shape independent of the bandwidth. Except for Ref. 13, all the calculations listed in Table I give values for φ between 4 and 5. We will see later that φ determines the most important features of the d-band Fermi surface.

TABLE I. The relative energies, in units of 0.001 Ry, of important states near the top of the d band, as obtained from a number of band calculations using muffin tin crystal potentials.

Element	Reference	Γ_{12}	X_5	W_1'	L_3	ΔE_r	ΔE_θ	φ
Cu	9	0	67	68	53	68	15	4.5
Cu	10	0	55	55	44	55	11	5.0
Fe	12	0	95	96	75	96	20	4.8
Ni	13	0	104	84	67	104	37	3.1
Ni	14	0	63	64	51	64	13	4.9

The bands surveyed in Table I are calculated in the paramagnetic state with no exchange splittings. To sketch the ferromagnetic bands it is necessary to estimate the exchange splitting of the s bands, ΔE_{ss}, and the exchange splitting of the d bands, ΔE_{dd}, when there are 0.6 unpaired d spins per atom.

Because the number of unpaired spins is nonintegral, Slater constructed[15] a band model for Ni with $\Delta E_{ss}=0$ and

$$\Delta E_{dd}=0.6\delta E_{dd}. \tag{2.2}$$

Here $\delta E_{dd}=0.8$ eV is an intra-atomic exchange integral between two d electrons in different atomic orbitals ($m\neq m'$). The attractive feature of Slater's theory is that when it is combined with the high density of states found[15] at the top of the d band (due to the small value of ΔE_θ), the one-electron energy difference between paramagnetic and ferromagnetic states is of the right order of magnitude to explain the Curie temperature.

The one-electron approach has been criticized by Van Vleck[16] on the grounds that in the crystal the interactions are much stronger than the $m'\neq m$ interactions in the free atom. This is because of quenching of the orbital angular momentum, which makes it possible for the one-electron orbitals to be more nearly alike. Then one should use a value for δE_{dd} intermediate between that of an $m\neq m'$ exchange integral (0.8 eV) and a screened Coulomb integral (an exchange integral with $m=m'$, of order 3–5 eV). When the total d-band width W (about 4 eV in Ni) is comparable to δE_{dd}, strong intra-atomic correlations are expected. These are supposed to explain the strong peak found[17] in the forward scattering of neutrons above the Curie tem-

[8] P. W. Anderson, Phys. Rev. **124**, 41 (1961).
[9] B. Segall, Phys. Rev. **125**, 109 (1962).
[10] G. A. Burdick, Phys. Rev. **129**, 138 (1963).
[11] J. C. Slater and G. F. Koster, Phys. Rev. **94**, 1498 (1954).
[12] J. H. Wood, Phys. Rev. **126**, 517 (1962).
[13] J. G. Hanus, MIT Solid State and Molecular Theory Group Quarterly Progress Report No. 44, p. 29, 1962 (unpublished).
[14] L. F. Mattheiss (to be published).
[15] J. C. Slater, Phys. Rev. **49**, 537 (1936).
[16] J. H. Van Vleck, Rev. Mod. Phys. **25**, 211 (1953).
[17] M. K. Wilkinson and C. G. Shull, Phys. Rev. **103**, 516 (1956).

perature. This peak has been thought to imply the persistence of short-range order among Heitler-London atomic spins when the exchange splitting is zero. However, Kubo *et al.*[18] have shown that the effect of short-range order above T_c can also be incorporated into a band model. At present the neutron studies do not appear to imply quantitative estimates for δE_{dd}.

We conclude that the original order-of-magnitude agreement obtained by Slater is still our best guide. We will see later that Fermi surface measurements may enable us to infer ΔE_{dd} experimentally, thereby resolving one of the many unclear aspects of ferromagnetism.

3. ALTERNATE FERMI SURFACE MODELS

From magnetoresistance[2] and Hall data,[3] one can infer that one sheet of the Fermi surface of Ni has the same topology as the s Fermi surface of Cu; i.e., it consists of spheroidal pieces connected by cylindrical necks through the centers of the L faces. The angle subtended by the necks, measured from Γ, is about 6°, compared to 20° for Cu.

The simplest model[19] for this sheet is to assume that the ↑ spin band is nearly the same as in Cu. The ↓ spin d band is partially filled, so that the unpaired electrons are in the ↑ spin d band, which is full. The important bands are shown schematically in Fig. 1(a); E_F falls just above $L_{2'}\uparrow$.

Two alternative models are proposed here. One [see Fig. 1 (b)], retains the $s\uparrow$ neck, but reduces substantially the energy difference between the neck and $L_3\uparrow$.

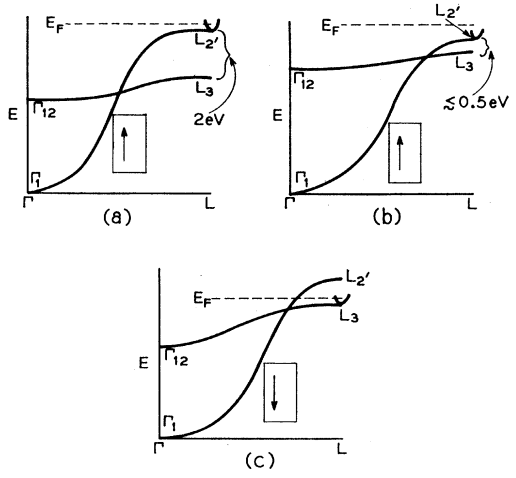

FIG. 1. Alternative models for the band structure of ferromagnetic Ni, with special reference to the neck found in galvanomagnetic experiments. For the sake of clarity, only the s-p band $\Gamma_1\Gamma_2$, and one twofold degenerate d band $\Gamma_{12}\Gamma_3$ are sketched. The neck is denoted by the "U" in each figure. The boxed arrows indicate spin direction; the unpaired electrons spins are ↑.

[18] R. Kubo, T. Izuyuama, D. J. Kim, and Y. Nagoka, J. Phys. Soc. Japan **17**, Suppl. B-I, 67 (1962); J. Phys. Soc. Japan **18**, 1025 (1963).

[19] H. Ehrenreich, H. R. Phillipp, and D. J. Olechna, Phys. Rev. **131**, 2469 (1963).

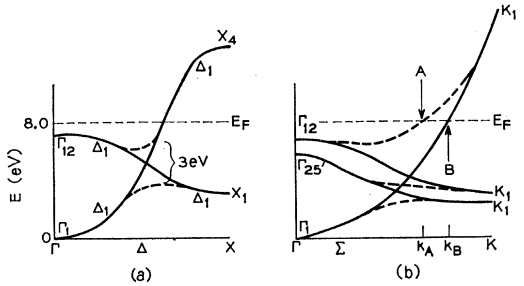

FIG. 2. The effects of s-d hybridization. The solid lines are s-p bands, Γ_1X_4 in (a), Γ_1K_1 in (b), or d bands, $\Gamma_{12}X_1$ in (a), or $\Gamma_{12}K_1$, $\Gamma_{25}'K_1$ in (b), without hybridization. The dashed lines show how the bands are affected by s-d interaction. For the sake of clarity only the d bands that interact with the s bands are sketched.

We will see that this is necessary to obtain an internally consistent model.

A second model places the neck in the $d\downarrow$ band, with E_F just above $L_3\downarrow$. This is shown in Fig. 1(c).

It has been emphasized that the Hall data unambiguously require three-electron Fermi surfaces (assuming that the $d\uparrow$ bands are full). The three surfaces are $s\uparrow$, $s\downarrow$, $d\downarrow$. The number of electrons in each surface per atom satisfy

$$n(s\uparrow)+n(s\downarrow)+n(d\downarrow)=1.0. \tag{3.1}$$

4. SATURATION MAGNETIZATION

The saturation number of Bohr magnetons per atom is 0.61. Combined with gyromagnetic g values[4] of 2.1, this gives

$$n(s\uparrow)+1.0-n(s\downarrow)-n(d\downarrow)=0.54. \tag{4.1}$$

Combining (3.1) and (4.1), we obtain

$$n(s\uparrow)=0.27. \tag{4.2}$$

5. GEOMETRY OF FERMI SURFACE MODELS

We consider quantitatively the three models shown in Fig. 1.

(a) The $s\uparrow$ surface is nearly identical to that of Cu. In Cu, E_F falls 0.75 eV above $L_{2'}$; from the neck dimensions E_F will fall at least 0.05 eV above L_2' in this model of Ni. Relative to Γ_1 we have $E_F=7$ eV. From the density of states measured for[20] Cu to a good approximation the number of $s\uparrow$ electrons is

$$n(s\uparrow)=0.50\ [1-2.1(\delta E/E_F)], \tag{5.1}$$

$$n(s\downarrow)=0.40. \tag{5.2}$$

Our result (5.2) differs by 25% from the value 0.33 calculated in Ref. 19. We conclude that the numerical methods used there are inaccurate. The difference between (4.2) and (5.2) leads us to suspect the validity of model (a).

Before passing to model (b), we consider the magnitude of effective magnetic fields at nuclei. According to

[20] B. W. Veal and J. A. Rayne, Phys. Rev. **130**, 2156 (1963).

Watson and Freeman,[21] the total $s\uparrow$ charge density probably does not exceed the total $s\downarrow$ charge density by more than 0.05 electrons/atom in Fe; we shall assume that this limit is valid for Ni as well.

The fundamental shortcoming of model (a) is that it places too many electrons in the $s\uparrow$ band. This can obviously be overcome by placing the neck in the d band, Fig. 1 (c). We shall now show that the neck in the $s\uparrow$ band can be retained by bringing the $d\uparrow$ band closer to E_F than it is in Cu.

(b) To treat the hybridizing or repulsive effect between s and d bands quantitatively, we note that for most radial variations of $\mathbf{k}$, there is a repulsion between the s and d bands similar to that shown in Fig. 2(b) for the low symmetry (110) direction. This repulsion reduces k_F from k_B to k_A. We may calculate $\delta k = k_B - k_A$ as a function of $E_F - \Gamma_{12}$ from the values of Ref. 13. The results are plotted in Fig. 3. We see that $\delta k \simeq 0$ for $E_F - \Gamma_{12} = 0.25$ Ry (the value appropriate to Cu).

We now assume that the s Fermi surface is spherical apart from cylindrical bulges along the [111] and [100] axes. Direct calculation shows that even when the (111) bulges touch to form necks of the observed size $n(s\uparrow)$ is augmented above its spherical value by less than 1%. Taking $\delta k_F/k_F$ from Fig. 3, we can calculate the volume Ω of an s sphere compared to $\Omega_0 = 0.50$ electrons/atom for Cu. This is also shown in Fig. 3. We note that in model (a) with E_F reduced by 0.05 Ry so that $E_F - \Gamma_{12} = 0.20$ Ry, $\Omega/\Omega_0 = 0.8$, in agreement with (5.2).

From (4.2) and Fig. 3 we obtain

$$E_F - \Gamma_{12}\uparrow = 0.12 \text{ Ry}. \tag{5.3}$$

In the $\downarrow$ band we must place E_F about 0.004 Ry below L_3 in order to obtain 0.54 unpaired spins.[15] According to Table I, $L_3 - \Gamma_{12} = 0.064$ Ry. This gives

$$E_F - \Gamma_{12}\downarrow = 0.06 \text{ Ry} \tag{5.4}$$

and enables us to estimate

$$\Delta E_{dd} = 0.6\delta E_{dd} = 0.8 \text{ eV}. \tag{5.5}$$

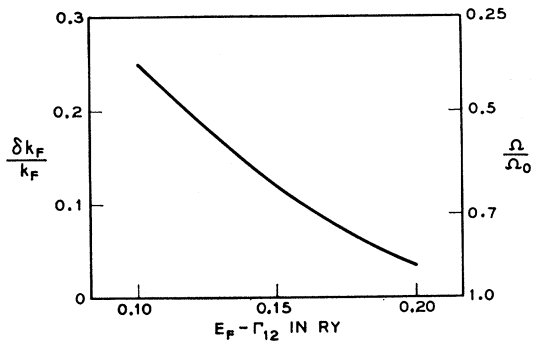

FIG. 3. The shrinking of s Fermi surfaces as a consequence of s-d interaction. Here $\delta k = k_B - k_A$, the latter being taken from Fig. 2(b).

[21] R. E. Watson and A. J. Freeman, Phys. Rev. **123**, 2027 (1961).

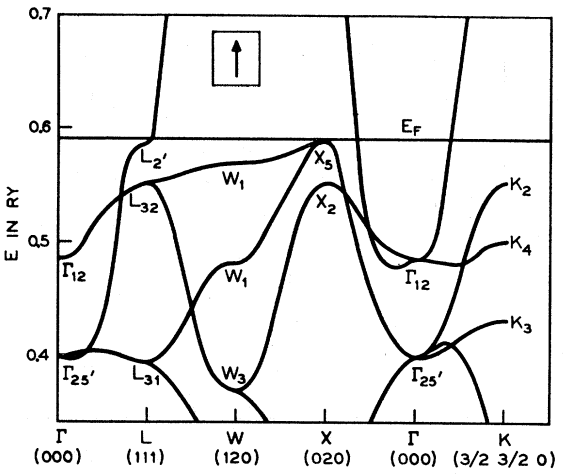

FIG. 4. The $\uparrow$ spin band structure of Ni in model (b).

According to Fig. 3 the value of $n(s\downarrow)$ associated with (5.4) is about 0.1, or about 0.15 less than $n(s\uparrow)$. This difference is apparently three times larger than that allowed by the effective nuclear magnetic fields.[21] In treating the effect of s-d repulsion on $n(s)$, however, we must remember that s-d hybridization is also present. This means that the s wave functions with nonzero amplitude at the nucleus are admixed into the lower d bands in Fig. 2(b). If the d bandwidth is neglected compared to the conduction bandwidth, one can show by a straightforward extension of the Anderson compensation theorem[22] that the difference between $n(s\uparrow)$ and $n(s\downarrow)$ is exactly compensated by the difference in s charge densities admixed into the respective d bands.

According to the compensation theorem, our limit on the difference of the total s charge densities can be used, in conjunction with (5.1), to place an upper limit on the exchange splitting of the s bands:

$$\begin{aligned} \Delta E_{ss} &\leq 0.05(E_F/1.2) \\ &\leq 0.4 \text{ eV}. \end{aligned} \tag{5.6}$$

The hybridization construction leading to (5.5) is quite crude and may be in error by 30%. Nevertheless, it is interesting to compare (5.5) with the estimate of ΔE_{dd} offered in Ref. 19 (2.0 eV) and by Slater[15] [0.5 eV, see (2.2)]. It appears that the exchange splitting estimated in Ref. 19 is too large by at least a factor of 2.

We have used the d-band shape given in Ref. 13 to sketch the d and s bands for model (b) in Fig. 4 ($\uparrow$ spin) and Fig. 5 ($\downarrow$ spin). Note in Fig. 4 that $L_{2'}$ lies 0.15 eV below E_F. This value will be justified in Sec. 6. In Fig. 5 we have placed $L_{32}\downarrow$ just above E_F, so that the $d\downarrow$ Fermi surface bulges towards the (111) faces but does not contact them in this model. The exchange splittings appropriate to these figures are

$$\Delta E_{ss} = 0.35 \text{ eV}, \quad \Delta E_{dd} = 0.50 \text{ eV}. \tag{5.7}$$

[22] P. W. Anderson (private communication).

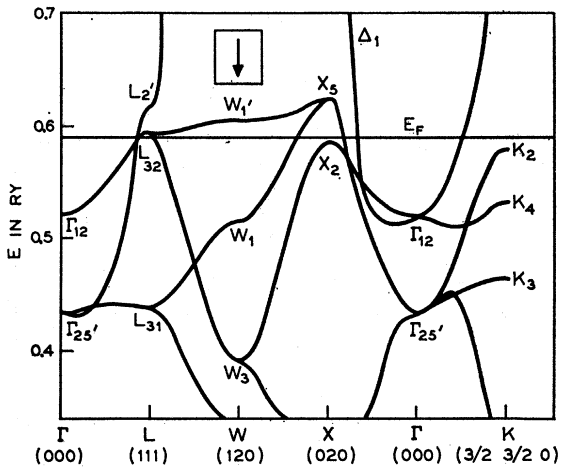

FIG. 5. The ↓ spin band structure of Ni in model (b).

(c) The foregoing analysis of the s Fermi surfaces is essentially unaltered if we assume that the neck falls in the $d\downarrow$ band with E_F slightly above $L_{32}\downarrow$ as shown in Fig. 1(c). The cylindrical bulges of the s surface along the [111] and [100] axes are reduced but, as we have remarked, these contribute negligibly to $n(s)$.

We have sketched all the d and s bands in Figs. 6 and 7 for model (c). The band values are taken from Ref. 13, with $\Delta E_{ss}=0$ and $\Delta E_{dd}=0.5$ eV. The $s\uparrow$ and $s\downarrow$ Fermi surfaces are spheroidal with slender bulges along [100] and [111] axes. The $d\downarrow$ Fermi surface consists of two inequivalent pieces. One of these is a spheriodal d piece; it lies entirely outside the s Fermi surface. The spheriodal d pieces are connected by (111) necks passing near L_{32} (the upper L_3 state). The second set of $d\downarrow$ Fermi surfaces are small pockets near the X_5 levels containing less than 0.05 hole/atom, which are neglected here.

From Fig. 7 we see that d necks require a low value for L_{32}, or a small value of φ defined by (2.1). The

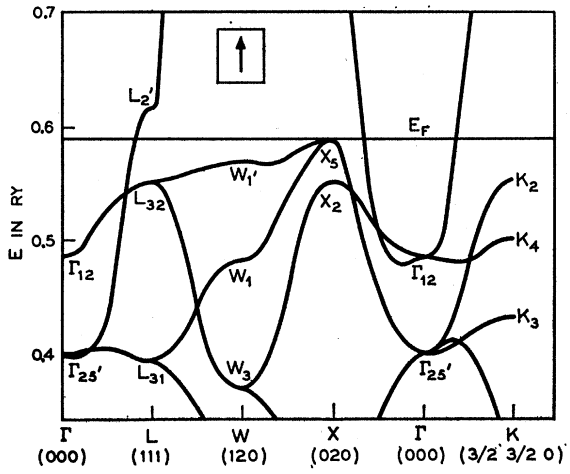

FIG. 6. The ↑ spin band structure of Ni in model (c).

value of φ obtained in Ref. 13 makes d necks feasible. On the other hand, the other values of φ listed in Table I do not appear to be compatible with d necks. (For $\varphi>4$, the d Fermi surface no longer contacts the (111) face, but instead becomes spheroidal.)

6. NECK GEOMETRY

To distinguish between models (b) and (c) we analyze the energy surfaces near L. With the usual $\mathbf{k}\cdot\mathbf{p}$ perturbation expansion, where $\mathbf{k}'=\mathbf{k}-\mathbf{L}$, we have, near the nondegenerate conduction band edge $L_{2'}$,

$$E_c(\mathbf{k})=E(L_{2'})+\frac{h^2}{2m_l}(k'_l)^2+\frac{h^2}{2m_t}(k'_t)^2. \quad (6.1)$$

In (6.1) the subscripts on k' specify its components parallel and perpendicular, respectively, to $\mathbf{L}$. The

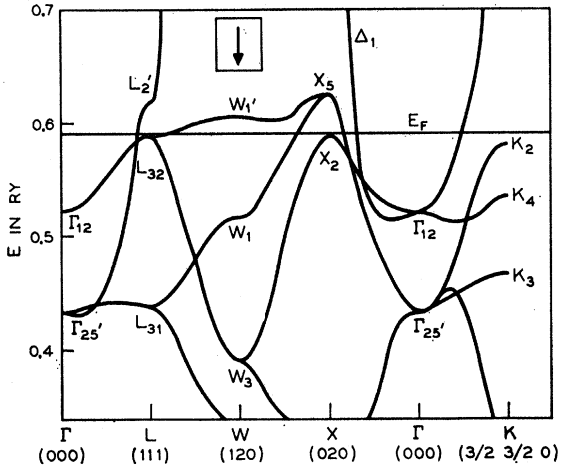

FIG. 7. The ↓ spin band structure of Ni in model (c).

longitudinal and transverse masses m_l and m_t are given by

$$\frac{m}{m_l}=1+\frac{2}{m}\sum_{j=L_1}\frac{|\langle L_1|p_l|L_{2'}\rangle|^2}{E(L_{2'})-E_j}, \quad (6.2)$$

$$\frac{m}{m_t}=1+\frac{2}{m}\sum_{j=L_3}\frac{|\langle L_3|p_t|L_{2'}\rangle|^2}{E(L_{2'})-E_j}. \quad (6.3)$$

The transverse mass m_t is dominated by $j=L_{32}$ and L_{31}. It has been calculated for Cu by Segall.[9] Assuming equal interband matrix elements, we find from Segall's calculated transverse mass

$$\frac{2}{m}|\langle L_{31}|p_t|L_{2'}\rangle|^2=\frac{2}{m}|\langle L_{32}|p_t|L_{2'}\rangle|^2=1.7\text{ eV}. \quad (6.4)$$

With $L_{2'}-L_{32}=0.3$ eV and $L_{2'}-L_{31}=2.4$ eV, from (6.3) and (6.4) we find for the s neck,

$$m_t=0.13m. \quad (6.5)$$

The lower L_1 state entering the sum in (6.2) is a d state. Assuming constant conduction-band, d-band matrix elements, from (6.4),

$$\frac{2}{m}|\langle L_1(d)|p_l|L_{2'}\rangle|^2=1.7\text{ eV}. \tag{6.6}$$

The upper L_1 state is just the usual $4s$-like state formed from the sum of $\exp(i\mathbf{L}\cdot\mathbf{r})$ and $\exp(-i\mathbf{L}\cdot\mathbf{r})$. The matrix element is estimated from the plane waves to be

$$\frac{2}{m}|\langle L_1(s)|p_l|L_{2'}\rangle|^2=\frac{2}{m}(\hbar L)^2=35\text{ eV}. \tag{6.7}$$

Combining (6.2), (6.6), and (6.7) with the calculated energy gaps,[13] we find

$$m_l=-0.25m \tag{6.8}$$

in good agreement with the value $-0.23m$ obtained directly from Segall's curve[9] for $E(\mathbf{k})$ along Λ.

The foregoing results can be refined quantitatively by calculating (6.4) as a function of

$$E_g=E(L_{2'})-E(L_{3j}). \tag{6.9}$$

The results of this calculation, which has been carried out by Mattheiss, are reported elsewhere.[23] When $E(\mathbf{k})-E(L_{2'})\gtrsim E_g/4$, fourth- and higher-order terms should also be included in (6.1). We neglect these here in the interest of simplicity.

Fawcett and Reed have estimated that the neck diameter in Ni is 3 times smaller than in Cu. Using (6.5) we obtain for model (b)

$$E_F-E(L_{2'}\uparrow)=0.15\text{ eV}. \tag{6.10}$$

The sum rules (6.2) and (6.3) are convenient for treating the s neck because only adjacent levels need be included in the sums. For the d bands, which have important interband matrix elements extending to high energies, this method is not appropriate. It is necessary to evaluate $E(\mathbf{k})$ for a d neck near $L_{32}\downarrow$ directly by solving the wave equation near L. Because of the twofold degeneracy of L_3 an expansion of the form (6.1) cannot be made rigorously. Qualitatively an expansion of the form (6.1) is valid for each of the two bands if we neglect the spin-orbit splitting at L_3. Each band has the same value for m_l. Transverse to $\mathbf{L}$ one has a heavy mass band and a light mass band. The transverse mass for the latter is given approximately by

$$\frac{m}{m_t(L_3)}=-\frac{m}{m_t(L_{2'})}+2, \tag{6.11}$$

where $m_t(L_{2'})$ is computed from (6.3). By using the augmented plane wave or APW method Mattheiss has computed[24] m_l and m_t for the heavy mass band. He finds

$$m_l/m=-3,\quad m_t/m=-8. \tag{6.12}$$

These masses are an order of magnitude larger than those near $L_{2'}$ estimated in (6.5) and (6.8). We note that the sign of m_t in (6.12) means that a d neck, as shown for model (c) in Fig. 7, is improbable. Although the expansion (6.1) is valid only very near L, an unusually rapid change in sign of m_t away from L would be required to explain the small neck radius found by Fawcett and Reed.[2,3] [*Note added in proof.* De Haas–Van Alphen studies of the neck geometry by A. S. Joseph and A. C. Thorsen (Phys. Rev. Letters **11**, 554 (1963), see also Ref. 23) rule out d necks.]

The qualitative survey that we have made here will now be of considerable use in interpreting optical data.

7. INTERBAND EDGES

Interband absorption edges have been found[19] at 0.3 1.4 eV. These have been assigned to transitions along symmetry lines near L.

In order to evaluate the significance of these assignments, it is again necessary to consider physically plausible rules. Inasmuch as the only completely successful analysis of interband structure has been carried out in semiconductors[25–28] (especially Si and Ge), we begin by discussing the methods there used.

The basic point is that in general the transitions may take place *anywhere* in the Brillouin zone. If we have a band model and fix $(E_n-E_{n'})$, then for a given pair of bands n and n' we still have to consider an energy surface which may extend throughout the zone.

We may still find edges, however, by looking for the Van Hove singularities[25,27] associated with interband critical points where

$$\nabla_{\mathbf{k}}[E_n(\mathbf{k})-E_{n'}(\mathbf{k})]=0. \tag{7.1}$$

Such critical points contribute corners to the imaginary part of the diagonal components of the dielectric tensor, ϵ^{ii}.

We propose here to identify interband edges in metals also with Van Hove singularities. It is useful to distinguish between two kinds of critical points

$$0\neq\nabla_{\mathbf{k}}E_n=\nabla_{\mathbf{k}}E_{n'}\quad\text{or}\quad 0=\nabla_{\mathbf{k}}E_n=\nabla_{\mathbf{k}}E_{n'}. \tag{7.2}$$

We refer to the former as general interband points (g.i.p.) and to the latter as symmetry interband points (s.i.p.).

In the case of Si and Ge about half the singularities were s.i.p.'s and half were g.i.p.'s. The s.i.p.'s of course occur at symmetry points, such as Γ, X, L, and W. Most of the g.i.p.'s occur along symmetry lines.

At first one could imagine that it is equally significant to identify a given edge as a s.i.p. or a g.i.p. If we com-

[23] J. C. Phillips and L. F. Mattheiss, Phys. Rev. Letters **11**, 556 (1963).
[24] L. F. Mattheiss (to be published).
[25] J. C. Phillips, Phys. Chem. Solids **12**, 208 (1960).
[26] J. C. Phillips, Phys. Rev. **125**, 1931 (1962).
[27] D. Brust, J. C. Phillips, and F. Bassani, Phys. Rev. Letters **9**, 94 (1962).
[28] F. Brust, M. L. Cohen, and J. C. Phillips, Phys. Rev. Letters **9**, 389 (1962).

pare Refs. 25 and 26 with Refs. 27 and 28, however, we notice that in the early work only s.i.p.'s were identified. This is because with g.i.p.'s there are so many possibilities that such an assignment is almost meaningless. Of course, when an exhaustive analysis of the interband density of states has located all the principal Van Hove singularities,[27,28] *then* one is justified in identifying g.i.p.'s as well as s.i.p.'s.

We now turn to a specific discussion of interband singularities in transition metals. As we remarked in Sec. 1, a good qualitative way of thinking of the band structure is in terms of decoupled $s-d$ bands. The d bands can be fitted by tight-binding expressions[11] using trigonometric functions with fundamental period equal to that of the Brillouin zone diameter. The d bandwidth is small (~ 4 eV). The s bands (~ 10 eV wide) can be fitted by nearly free-electron expressions. Under these circumstances we ordinarily have $|\nabla_k E_d(\mathbf{k})| \ll |\nabla_k E_s(\mathbf{k})|$. Thus, kinks responsible for g.i.p.'s in semiconductors (e.g., the $\Lambda_3 \rightarrow \Lambda_1$ g.i.p. in[27] Ge) are much less likely in $d \rightarrow s$ transitions. If possible we should assign our interband edges to the symmetry points Γ, X, L, or W.

There is one difference between metals and semiconductors which is important here. Because of the exclusion principle transitions between bands n and n' may be allowed over only part of the Brillouin zone in metals. If the boundary of the allowed region passes near the critical point the strength of the Van Hove singularity may be altered.

The 0.3-eV interband edge has been assigned[19] to transitions between the $\downarrow$ conduction and d bands along the symmetry lines Λ or Q in the general neighborhood of L. We have analyzed the energy surfaces near L by $\mathbf{k}\cdot\mathbf{p}$ perturbation theory (see Sec. 6) and found that a Van Hove interband singularity of the M_1 (saddle point) type occurs at L. There is *no* g.i.p. along Λ or Q near L; indeed, it can be shown that because of the saddle point nature of the singularity Λ and Q are relative *minima* for the interband density of states.

To illustrate our analysis we show in Fig. 8 the contours of constant interband energy near L. (The results are qualitatively the same for both of the d bands which belong to L_3.) Near L the surfaces determined by

$$E_c(\mathbf{k}) - E_d(\mathbf{k}) = E(L_{2'}) - E(L_3) \qquad (7.3)$$

are cones with apex at L. The joint density of states has an edge at this energy difference because of the high density of states associated with the conical surface.

The effect of the exclusion principle on the $\uparrow$ interband transitions is shown in Fig. 8(a). Interband transitions are allowed outside the boundary curves marked E_F. The conduction band states near $L_{2'}\uparrow$ are filled in model (b) inside these boundary curves. The conical surface (7.3) does not contribute to $\uparrow$ interband transitions. This figure is qualitatively valid for transitions between either of the d bands degenerate at L_3 and the conduction band near $L_{2'}$.

For transitions between $\downarrow$ bands we consider only transitions between the light mass d band and the conduction band. The density of states in the d band has been studied by several authors.[15,29] The density of states shown in Fig. 9 is a smoothed histogram of these results.[29] We emphasize the M_1 edge in dN/dE due to L_{32}.

All previous workers[15,29,30] have found that for the $d\uparrow$ band to contain about 0.6 unpaired spins the Fermi energy in the $d\downarrow$ band must be given by

$$\delta = E(L_{32}\downarrow) - E_F \lesssim 0.05 \text{ eV}. \qquad (7.4)$$

This value of δ is much smaller than the one assumed in Ref. 19 (0.24 eV). The latter value leads, as shown in Fig. 9, to 1.2 unpaired spins (not 0.7, as inferred by inaccurate numerical methods[19]). We shall now demonstrate that the optical data provide a precise confirmation of (7.4).

When the equality sign holds in (7.4) a long, narrow cylinder along Λ does not contain d electrons and does not contribute to interband transitions. This is the situation in model (b); the forbidden region lies inside E_F in Fig. 8(b). In model (c) we have L_{32} below E_F and

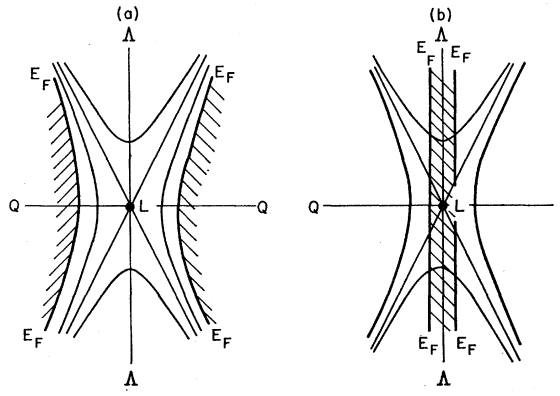

FIG. 8. Interband transitions near L. Surfaces of constant interband energy $E_{cd} = E_c(\mathbf{k}) - E_d(\mathbf{k})$ are shown in the plane. (a) The curves for $\uparrow$ bands are shown together with the boundary curves labeled E_F, which mark the position of the Fermi energy in the conduction band, $E_c(\mathbf{k}) = E_F$. Interband transitions are allowed in the shaded region. (b) The curves for $\downarrow$ bands together with the boundary curves labeled E_F, which mark the position of the Fermi energy in the d band $E_d(\mathbf{k}) = E_F$. Interband transitions are allowed in the unshaded region outside the boundary curves.

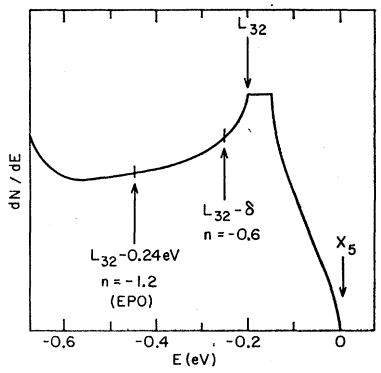

FIG. 9. The smoothed density of states in the $\downarrow$ d band, after Ref. 29. The position of E_F required to give 0.6 unpaired spins is indicated, as are also the position of $L_{32}\downarrow$ and the position of E_F used in Ref. 19.

[29] G. F. Koster, Phys. Rev. **98**, 901 (1955).
[30] G. C. Fletcher, Proc. Phys. Soc. (London) **A65**, 192 (1952).

there is no forbidden region for the light mass band. In this case (7.4) holds automatically. Case (b) is more interesting.

In this case most of the conical surface lies outside the forbidden cylinder and we expect a strong interband edge near $E_g=E(L_{2'}\downarrow)-E(L_{32}\downarrow)$. To see whether the forbidden region shifts the edge appreciably we have evaluated the joint density of states function

$$\frac{dN}{dE_{cd}}\sim\int\frac{dS}{|\nabla_k E_{cd}|} \tag{7.5}$$

near L for $E_{cd}(\mathbf{k})=E_c(\mathbf{k})-E_d(\mathbf{k})$ given by the expressions for the conduction band and the light mass d band discussed in Sec. 6. We find

$$\frac{dN}{dE_{cd}}=C-C'(2\delta)^{1/2},\ E_{cd}\geq E_g \tag{7.6}$$

$$=C-C'(2\delta+E_g-E_{cd})^{1/2},\ E_{cd}\leq E_g, \tag{7.7}$$

which reduces to the usual result for an M_1-type singularity when $\delta=0$. The edge associated with (7.6) and (7.7) appears to be shifted away from E_g by $\delta\lesssim 0.05$ eV, a negligible effect. We conclude that the interband edge observed[19] at 0.3 eV can be assigned to $E(L_{2'}\downarrow)-E(L_{32}\downarrow)$.

In order to display the character of the 0.3 eV interband edge more clearly, we have separated the contributions to $\epsilon_2{}^{ii}$ into parts associated only with the conduction band and a residue associated with the d band. The former is assumed to be the same in Ni as in Cu. The latter can then be obtained by subtracting ϵ_2(Cu) from ϵ_2(Ni). The result obtained from the data[19] is shown in Fig. 10. The M_1 nature of the edge, as described by (7.6) and (7.7), is striking. Furthermore, the inequality (7.4) must hold. [The value $\delta=0.24$ eV (used in Ref. 19) is incompatible with the line shape of Fig. 10.]

The size of the forbidden region in Fig. 8(b) is large enough to make it difficult but not impossible to resolve the spin-orbit splitting of the L_3 level. The atomic spin-orbit splitting, $\zeta_{3d}=0.07$ eV,[31] is somewhat larger than δ. Lifetime effects may prevent the observation of the spin-orbit splitting; we therefore discuss an experiment closely related to the spin-orbit splitting in the next section.

With regard to the 1.4-eV interband edge, we consider the difference between this energy and the calculated value of $(W_1,W_{1'})=1.1$ eV to be within the range of uncertainty of the band calculation.

8. FARADAY RESONANCES

Rotation of the plane of polarization of either transmitted or reflected light is described by the off-diagonal components ϵ^{ij} of the dielectric tensor. Argyres[32] has shown that such components are obtained through spin-orbit mixing of the $\uparrow$ and $\downarrow$ wave functions. He also remarked that a reversal of sign of the imaginary part $\epsilon_2{}^{ij}$ can be obtained if the interband energy density is peaked. We note that such a peak or edge in $\epsilon_1{}^{ij}$ will also be obtained from Van Hove singularities. We refer to such a peak as an interband Faraday resonance.

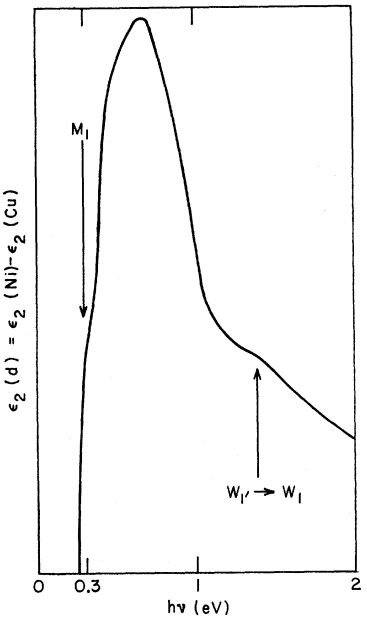

FIG. 10. The contribution to ϵ_2 in Ni due to the d bands alone, which below 2 eV is approximated by ϵ_2(Ni)−ϵ_2(Cu).

A special case of interband Faraday resonances associated with the direct transition threshold (interband minimum of type M_0) has been analyzed in some detail for semiconductors.[33,34] The first important point to note is that ϵ^{ij} is proportional to $(\delta g_n-\delta g_{n'})$, the difference in g shifts of the two bands. The latter is due to the spin-orbit splitting of orbitally degenerate levels. The source of the Faraday resonance is therefore formally the same in ferromagnetic metals, normal metals, and semiconductors, contrary to the assertions of Ref. 19. Although the theory for semiconductors[33] has been developed in terms of Landau levels, semiclassical orbital quantization is merely a convenient tool for handling the matching of interband energies. The resonance is a matching in k space, not in time; the condition for well-resolved resonance is $\omega_{nn'}\tau\gtrsim 1$, not $\omega_c\tau\gtrsim 1$ (ω_c is the cyclotron frequency).

It appears that Faraday resonances in $\epsilon_1{}^{ij}$ will be quantitatively different from the Van Hove singularities in $\epsilon_2{}^{ij}$. Consider s.i.p.'s. If we have an interband threshold of the M_0 type, then the energy contours will be closed surfaces near the symmetry point and $\delta g_{nn'}=\delta g_n-\delta g_{n'}$ averaged over such a surface will be nearly the same for all surfaces. However, if the singularity is of the M_1 type we may expect that $\delta g_{nn'}$ will vary appreciably over the conical surface passing through the symmetry point (see Fig. 8). In fact far from the sym-

[31] E. O. Condon and G. H. Shortley, *The Theory of Atomic Spectra*, (Cambridge University Press, New York, 1957).
[32] P. N. Argyres, Phys. Rev. **97**, 334 (1955).
[33] I. M. Boswarva, R. E. Howard, and A. B. Lidiard, Proc. Roy Soc. (London) **A269**, 125 (1962).
[34] I. M. Boswarva and A. B. Lidiard, in *Proceedings of the International Conference on the Physics of Semiconductors Exeter* (The Institute of Physics and the Physical Society, London, 1962).

metry point (or line) of orbital degeneracies, we should have $\delta g_{nn'} \to 0$. These quantitative differences suggest that Faraday resonances may be a tool which can play the same decisive role in interpreting crystal spectra that the Zeeman effect has played in atomic and molecular spectra. In any case the Faraday resonances which have been observed in Ni[5] at 0.3 eV and 4.1 eV are more informative than spin-orbit splittings which have yet to be resolved at these energies. Further insight into Faraday resonances could easily be obtained by studying the well-separated $L_{3'} \to L_1$ and $\Lambda_3 \to \Lambda_1$ singularities in GaAs or GaSb.[35]

From the foregoing discussion it is evident that we identify the Faraday resonance at 0.3 eV in Ni with the $(L_{32}\downarrow) \to (L_{2'}\downarrow)$ energy cone responsible for the interband edge. With no Van Hove singularities along Λ or Q we find no reason for supposing[19] otherwise.

9. CONCLUSIONS

We have examined a variety of experimental evidence. We summarize here the conclusion which can be drawn from the analysis.

(A) There are two possible locations for the (111) necks. These are in the conduction band near $L_{2'}\uparrow$ or in the d band near $L_{32}\downarrow$. All the evidence tends to favor $L_{2'}\uparrow$, model (b). This point can be definitely settled once the effective masses are known, because the effective masses in the d band are an order of magnitude larger than in the conduction band.

(B) The data shed more light than one might have anticipated on the position of E_F in the $\uparrow$ and $\downarrow$ bands:

(1) If the neck is in the conduction band near $L_{2'}\uparrow$, then the $\uparrow d$ bands must be much closer to E_F than in Cu. The quantitative development of this argument led to an estimate in Sec. 3 for the exchange splitting of the d bands,

$$\Delta E_{dd} \lesssim 0.8 \text{ eV}. \tag{9.1}$$

(2) In the $\downarrow d$ bands the Fermi energy required to give the correct number of unpaired spins is[15,29,30]

$$E_F = E(L_{32}\downarrow) - \delta, \tag{9.2}$$

with $\delta \lesssim 0.05$ eV. We have shown that this value of δ is consistent with the optical data, and that a much larger value (say[19] 0.24 eV) is not. This shows that the optical data can provide a quantitative check on the calculated shape of the d bands in a *specific* neighborhood of k space which also sheds light on the over-all shape of the bands.

(C) From the Anderson compensation theorem[8] an upper limit can be placed on the exchange splitting of the conduction band

$$\Delta E_{ss} \lesssim 0.4 \text{ eV}. \tag{9.3}$$

[*Note added in proof.* New data has come to our attention which agrees well with the $L_{2'}$ and L_{32} bands as sketched in Fig. 1(b) and Fig. 4.

Consider first $\epsilon_2(d)$ as sketched in Fig. 10. In addition to the previously identified peaks near 0.3 and 1.4 eV there is a broad peak near 0.6–0.7 eV. Because of the large Drude background the subtraction procedure used to obtain $\epsilon_2(d)$ is uncertain. Nevertheless, it is reasonable to suppose that $\epsilon_2(d)$ below 1 eV consists of two similar superimposed absorption peaks of approximately equal strength, with maxima at 0.3 and 0.6 eV. The former peak is identified with transitions near the $(L_{32}\downarrow, L_{2'}\downarrow)$ bands [Fig. 8(b)], while the latter can only be assigned to $(L_{32}\uparrow, L_{2'}\uparrow)$ as shown in Fig. 8(a).

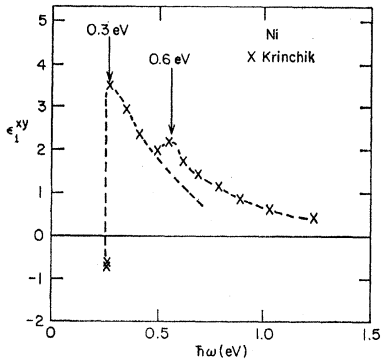

FIG. 11. The real part of the off-diagonal component of the dielectric tensor ϵ_1^{xy} with M along the z axis as a function of photon energy $\hbar\omega$, according to Krinchik.

If this interpretation is correct, then we should expect a peak in ϵ_1^{ij} not only at 0.3 eV but also at 0.6 eV. Krinchik (1963 Conference on Magnetism and Magnetic Material, to be published in J. Appl. Phys.) has measured ϵ_1^{ij} between 0.25 and 1.0 eV. His original experimental points are shown in Fig. 11. At 0.6 eV there is a well-defined peak similar in shape to the 0.3 eV peak, as expected. We have indicated the decomposition of the structure into two peaks by dashed lines.

The interesting feature of this decomposition is that in ϵ_1^{ij} the 0.6 eV peak is about 5 times weaker than the 0.3 eV peak, whereas in ϵ_2^{ii} the two are of comparable magnitude. According to the discussion of Sec. 8, we expect $\delta_{g_{nn'}}$ to be especially large near the line of orbital degeneracy for the Λ_3 states. According to Fig. 8 we expect δ_g averaged over the constant interband energy surfaces to be much smaller for the $\uparrow$ bands than for the $\downarrow$ bands, because much more of the region near is excluded from contributing to the $\uparrow$ interband transitions. Note that this reinforces our conclusion about the smallness of δ as given by (9.2).

For practical purposes we may set $|\delta| \leq 0.1$ eV. Then the exchange splitting ΔE_{dd} is given directly by the interband energy required for transitions from the heavy mass (nearly flat) $L_{32}\uparrow$ band to the bands near $L_{2'}\uparrow$ at E_F. This is just 0.6 eV according to Fig. 11. The value

$$\Delta E_{dd} = (0.6 \pm 0.1) \text{ eV}$$

is quite consistent with the conclusions stated in (9.1) and in Ref. 23.]

ACKNOWLEDGMENTS

I have benefited from conversations with P. W. Anderson, V. Heine, and L. F. Mattheiss. I am particularly grateful to Dr. H. Ehrenreich for a preprint of Ref. 19. The kind hospitality of the Cavendish Laboratories, Cambridge, and Bell Laboratories during the preparation of this paper is appreciated.

[35] J. C. Phillips, Phys. Rev. 133, A452 (1964).